JOURNAL OF MATERIALS SCIENCE 20 (1985) 1645–1659

A model for the compressive buckling of extended chain polymers

STEVEN J. DeTERESA, ROGER S. PORTER, RICHARD J. FARRIS
Materials Research Laboratory, Polymer Science and Engineering Department, University of Massachusetts, Amherst, Massachusetts 01003, USA

A model for the compressive buckling of an extended polymer chain is presented. The application of classical elastic instability analysis to an idealized polymer chain reveals that the bending rigidity and critical buckling loads for a chain are proportional to the force constants for valence bond angle bending and torsion. Highly oriented polymer fibres are treated as a collection of elastic chains that interact laterally. The critical stresses to buckle this collection of chains are calculated following a procedure developed to predict the compressive strengths of fibre-reinforced composites. This buckling stress is predicted to be equal to the shear modulus of the fibres and is the limiting value of compressive strength. Comparison of experimental and predicted values shows that the theory overestimates the compressive strength, but that there is a correlation of shear modulus with axial compressive strength. Consideration of flaws in both the theory and the material indicate that the compressive strength should be proportional to either the shear modulus or shear strength of the fibres.

Nomenclature

P = axial compressive load (force)
P_{cr} = critical buckling load (force)
M, M_i = bending moments
l = length of a link
p = number of links
k = elastic hinge constant
α, α_i = angular rotation of hinges
L = overall chain or column length
v, v_i = lateral deflection of buckled chain or column
x, y, z = Cartesian coordinate axes
E = Young's modulus of isotropic column
I = moment of inertia
a_{ij} = matrix coefficients
A_p = coefficient for exact buckling loads of chains
ΔT = energy change due to work of external load on buckled column or chain
ΔU_1 = bending strain energy change of buckled column or chain
$\Delta U_2, \Delta U_2^e, \Delta U_2^s$ = strain energy changes in elastic foundation, where e refers to extension mode buckling and s refers to shear mode buckling
E_t = transverse modulus
G = longitudinal shear modulus
b = dimension associated with chain packing
A = cross-sectional area per chain ($= b^2$)
$f(x)$ = curve fitted to shape of buckled chain
m, n, r = integers
a_n = coefficients of trigonometric series
ϵ_y = normal strain in y-direction
σ_y = normal stress in y-direction
γ_{xy} = shear strain in xy plane
τ_{xy} = shear stress in xy plane
u_x = displacement in x-direction
u_y = displacement in y-direction
V = volume

0022–2461/85 $03.00 + .12

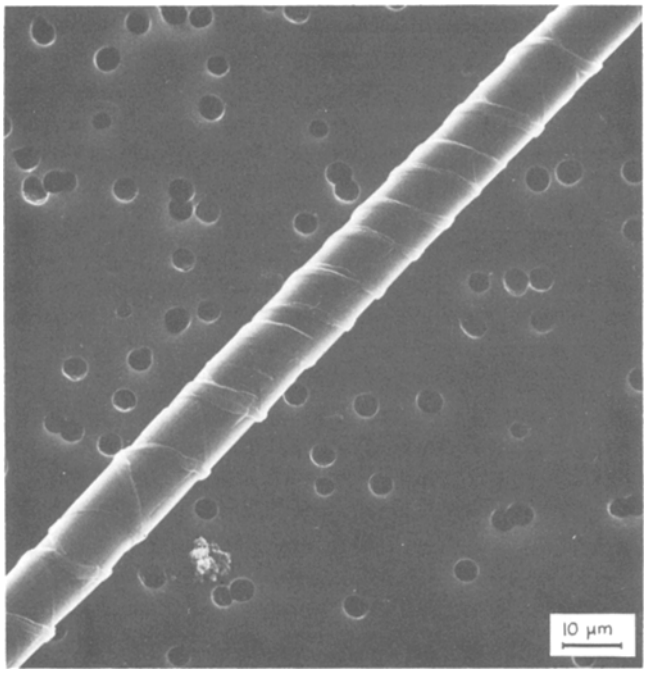

Figure 1 Compressive kink bands in Kevlar 49 fibre.

1. Introduction

Structure–property relationships are highly important for oriented polymers. Such polymers typically have a relatively large axial modulus and small transverse and shear moduli. This behaviour can be accounted for by strong covalent bonding along the chain orientation axis, and weaker secondary bonds between chains. The directionally dependent bond strengths are also evident in the disparity between large axial tensile strengths and smaller transverse tensile and shear strengths. Furthermore, the axial compressive strengths of oriented polymers are typically less than 25% of their corresponding tensile strengths. Because highly oriented polymers are becoming attractive as structural materials, the low compressive strengths of these materials have become a major concern. The reasons for this relative weakness in compression are not clear. In this paper a mechanism for buckling of highly oriented polymers during axial compression is proposed. A model is introduced that allows both predictions of compressive strengths and perhaps some understanding of the failure process.

2. Background

Compression of oriented polymers along the orientation axis results in an apparent failure which manifests itself as kink band formation An example of kink banding in axially compressed Kevlar fibres is shown in Fig. 1, These compressive kink bands have been observed for well-oriented polymers based on both rigid rod [1–6] and flexible [7–15] chains. Most of these polymers exhibit nearly linear elastic behaviour in compression until the onset of kink banding. This point usually coincides with a maximum compressive load and the initiation of inelastic deformation. The compressive strength of these oriented polymers is usually defined as the stress which initiates the apparent yield behaviour and concommitant kink banding. These compressive characteristics are not unique to oriented polymers, having been observed for other materials exhibiting similar structural anisotropy such as wood [16, 17], unidirectionally reinforced fibre composites [18–22], graphite fibres [23, 24] and models of foliated rock [25].

The compressive strength of fibre-reinforced materials has been analysed with regard to elastic instabilities [26–29]. These theories predict the compressive strength to be the critical load necessary to cause the microbuckling of a system of parallel and stiff fibres in an isotropic and elastic matrix. The most frequently cited analysis is by Rosen [26], who used energy methods developed by Timoshenko and Gere [3] to solve the problem of buckling of columns supported by an elastic foundation. The compressive strengths predicted by this theory are typically twice the experimental

values for well-fabricated composites reinforced with isotropic fibres such as boron [31]. The discrepancy between measured and predicted values has been attributed to use of a two-dimensional instability model to predict compressive strength for a material which is three-dimensional. The predicted strengths represent upper bounds, and in many cases the measured compressive strengths of composites are much lower than half the values predicted by stability analysis. The reasons postulated to account for these discrepancies include imperfections (voids, poor fibre packing and alignment, poor fibre–matrix adhesion, etc.) and inelastic behaviour of either matrix or fibre. Other theories have subsequently been proposed to predict compressive strengths when these effects are included in the analysis (see, for instance, [32, 33] for reviews of fibre composite compressive strength theories). A prevailing result in many of these theories is the proportionality of compressive strength with either longitudinal shear moduli (for "failure" as predicted by elastic instabilities) or longitudinal shear strengths (for shear failure instabilities).

Analyses of the compressive strengths of oriented polymers have been focused on continuum mechanics treatments of anisotropic yield behaviour [11], the analysis of deformation along preferential slip planes [4, 7, 9, 11, 13, 15], or dislocation models for kink formation [34]. The bulk of this work indicates that failure in compression results from shear deformation or slippage between polymer chains. However, to our knowledge there are no general theories based on molecular concepts which predict the axial compressive strengths of highly anisotropic polymers.

The morphology of kink bands formed in oriented polymers is strikingly similar to that of kink bands observed in the axial compression of fibre composites. Furthermore, we have shown that the permanent damage sustained by Kevlar fibres during kink formation is minimal and that compressive failure appears to be the result of buckling of microstructural elements [5]. The concept of microbuckling under compression has been proposed for carbon fibres [23, 24], oriented polyethylene [10] and Kevlar fibres [1, 2, 5].

The similarities between fibre composites and oriented polymers have led us to consider the concept of failure due to microbuckling instabilities for extended polymer chains subjected to axial compression. In this work a simple mechanical model is used to predict the compressive buckling loads of a single long and stiff polymer chain. Analysis of this model leads to a relationship between the bending stiffness of an extended chain and the force constants for bond angle deformations. The results for a single chain are then applied to a collection of such chains that interact through lateral bonding. The load required to buckle this collection of oriented chains is calculated as an estimate of the compressive strength of highly oriented polymers. The interaction between chains is accounted for in much the same way that Rosen approached the problem of predicting the compressive strengths of fibre composites using the energy methods outlined by Timshenko and Gere. Finally, the predictive power of this simple and ideal model is tested against experimentally determined compressive strengths of highly oriented polymer fibres.

3. Rigid-link–elastic hinge model for single extended polymer chain

The mechanical modelling of chemical bonds between atoms and molecules with springs has been a popular concept (refer to any standard Physical Chemistry text). Indeed, the calculations of theoretical moduli of extended polymer chains involve treating the chain as a series of elastic springs connected by elastic hinges. One of the first calculations of axial modulus of long chain molecules was made by Mark [35], and since then has been performed by many others for several polymers. Force constants for the springs and hinges are obtained from infrared spectroscopy measurements of force constants for bond stretching and bond angle bending, respectively. For small deflections about equilibrium positions, the bonding potential energy profile is assumed to be parabolic so that forces are proportional to deflections. This assumption of linear springs results in equivalent calculated tensile and compressive moduli.

Under compression, a long and stiff polymer chain can buckle in a manner similar to the buckling of a long slender column. Buckling of a chain can occur by contraction of bonds, bending of bond valence angles, and/or bond rotation (torsion). Even if these deformations were only slight deviations from equilibrium positions, the summation of them all along a large section of the chain could result in significant chain axis curvature. The force

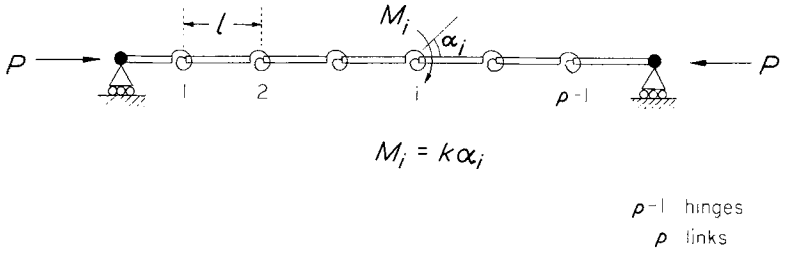

Figure 2 Schematic representation of link–hinge chain.

constants for each type of deformation provide a measure of the resistance of an extended chain to buckling and the total effect could be considered a "bending stiffness" of the chain. If it is possible to obtain a measure of this bending stiffness, then the application of classical instability analysis can provide an estimate of the compressive load required to initiate chain buckling.

As in calculations of theoretical moduli, buckling loads are calculated for static conditions by assuming bond lengths, bond angles, and force constants remain at their respective equilibrium values. The actual values of equilibrium bond lengths and angles, and the orientations of bonds with respect to the chain axis differ for each polymer. To take these specific geometric factors into consideration is beyond the scope of this paper. It is emphasized that consideration of these factors will improve the predictive power of the model, but to introduce the concept of elastic buckling instabilities in fully extended polymer chains under axial compression, the following simplifying assumptions will be applied to the model. The polymer chain consists of rigid links of equal length, l, oriented along the chain axis. Furthermore, the links are connected by linear elastic hinges of equal stiffness, k. A representation of the model is shown in Fig. 2.

Covalent bonds have been replaced with rigid links for two reasons. First, tabulated values of force constants indicate that bond stretching constants are at least an order of magnitude greater than torsion and bending constants [36, 37]. Therefore, most of the deformation in a loaded chain is primarily due to bond angle changes. Second, the axial deformation of a buckled chain is negligible compared to the displacement due to bending the chain. This assumption of "axial rigidity" is also made in the classical analysis of column buckling.

The elastic hinges represent the bending of valence bond angles and bond rotation. If bending deflections are small, the hinges can be considered linear elastic. The bending moment developed at any hinge is then equal to the product of k and the angular rotation, α, as shown in Fig. 2.

To calculate critical buckling loads for the link–hinge chain, one approach is to perform a static equilibrium analysis of the system in the buckled configuration and determine the minimum value of compressive load required to maintain such an equilibrium. It is assumed that the chain is pinned at its ends (i.e., no reaction moments) and that the compressive load is conservative. Additionally, at the onset of buckling the magnitude of the lateral deflections are assumed to be small relative to the overall chain length and confined to a single plane, thereby reducing the problem to two dimensions.

The equations obtained from a static equilibrium analysis of bending moments at each hinge of the buckled chain form a set of $p - 1$ linear and homogeneous algebraic equations for a chain with p links. This set of equations can be written in matrix form as,

$$\begin{bmatrix} a_{11} & a_{12} & a_{13} & \cdots & a_{1,p-1} \\ a_{21} & a_{22} & a_{23} & \cdots & a_{2,p-1} \\ \cdot & & & & \cdot \\ \cdot & & & & \cdot \\ \cdot & & & & \cdot \\ a_{p-1,1} & a_{p-1,2} & a_{p-1,3} & \cdots & a_{p-1,p-1} \end{bmatrix} \begin{bmatrix} \alpha_1 \\ \alpha_2 \\ \alpha_3 \\ \\ \alpha_{p-1} \end{bmatrix} = \begin{bmatrix} 0 \\ 0 \\ 0 \\ \\ 0 \end{bmatrix} \tag{1}$$

TABLE I Comparison of critical loads calculated from exact equilibrium analysis and from approximate formula for long link–hinge columns

p	A_p	$(\pi/p)^2$	$\frac{A_p}{(\pi/p)^2}$
2	2	2.467	0.81
3	1	1.097	0.91
4	0.586	0.617	0.95
5	0.382	0.395	0.97
6	0.268	0.274	0.98

$P_{cr}^{exact} = A_p(k/l)$
$P_{cr}^{approx.} = (\pi/p)^2(k/l)$

where the angles α_i are the rotation of each hinge i and the coefficients a_{ij} are functions of the compressive load, P, the hinge constant, k, and the length of a link, l.

The calculation of buckling loads is an eigenvalue problem for this set of linear equations. The $p-1$ eigenvalues obtained from the nontrivial solution of Equation 1 are the compressive loads which cause buckling. The minimum positive eigenvalue is the critical buckling load P_{cr}. An example of these calculations for a chain with $p = 4$ is given in Appendix 1.

The calculated critical loads for any value of p are all of the form;

$$P_{cr} = A_p \left(\frac{k}{l}\right) \tag{2}$$

where the coefficient A_p is a function of p only. Values of A_p for $p = 2$–6 are given in Table I. These results show that the critical buckling load decreases with increasing chain length.

In performing the calculations of critical loads by moment equilibrium analysis, it becomes evident that the computation difficulty increases rapidly with increasing model size. In other words, for a chain with p links the determinant of a $(p-1) \times (p-1)$ matrix must be found and after setting this determinant equal to zero, the $(p-1)$ roots of the resulting polynomial must be determined. So that the buckling analysis may be applied to polymer chains where p is very large, we seek to derive a single relationship between the critical buckling load and the values p, k, and l.

4. Approximate buckling load formula for long link–hinge chains

Intuitively, it appears that the buckled shape of a long link–hinge chain (p large) should be similar to the shape of a buckled elastic column of the same length and with the same end restraints. This analogy is illustrated in Fig. 3.

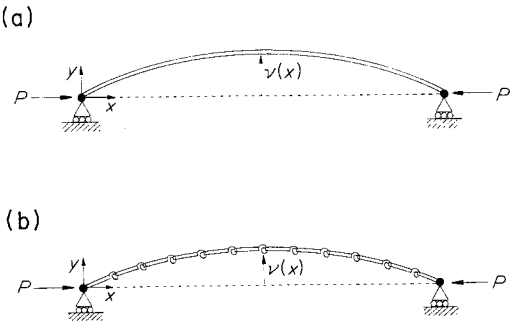

Figure 3 Buckled shapes of an elastic column and a long link–hinge chain.

The bending moments in a loaded elastic column are related to material properties by the equation:

$$EI\frac{d^2\nu}{dx^2} = M(x) \tag{3}$$

The critical load for the buckling of an elastic column can also be calculated using a static equilibrium analysis of the buckled column. Referring to Fig. 3, it can be seen that the bending moment at any point along the column is given by:

$$M = -P\nu. \tag{4}$$

Substituting this result into Equation 3 and rearranging yields:

$$EI\frac{d^2\nu}{dx^2} + P\nu = 0. \tag{5}$$

Solutions to this differential equation lead to discrete values of the load, P, required to initiate buckling. The minimum (critical) value for a column with pinned ends is known as the Euler buckling load and is given by:

$$P_{cr} = \frac{\pi^2 EI}{L^2}. \tag{6}$$

The next task is to demonstrate the analogy between Euler buckling of a continuous column and buckling of the link–hinge chain when the number of elements is large. This will be accomplished by deriving a "differential equation" for static equilibrium of the link–hinge chain and comparing it to Equation 5.

A coordinate system for the buckled configuration of the link–hinge chain is defined as shown in Fig. 4a. The balance of bending moments at any

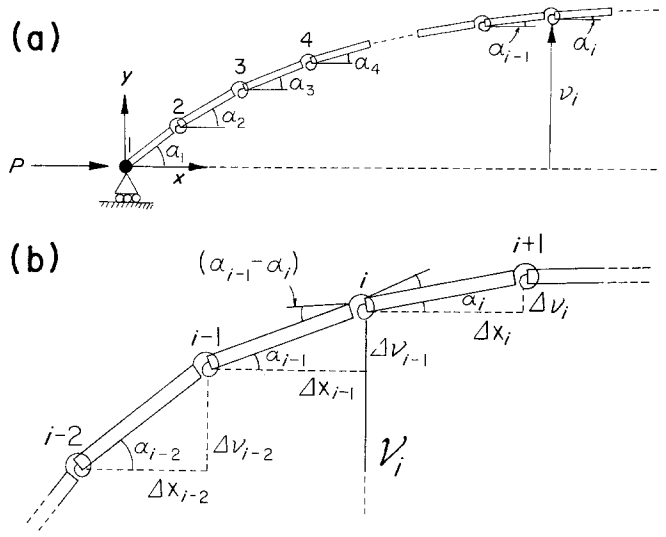

Figure 4 (a) Coordinates to describe shape of buckled link–hinge chain. (b) Expanded view in vicinity of hinge i.

arbitrary hinge, i, is given by:

$$\Sigma M = Pv_i - M_i = 0, \tag{7}$$

where v_i is the lateral deflection of hinge i from the x-axis. The bending moment, M_i, is due to the rotation of hinge i from its equilibrium position. By inspection of an expanded view of the buckled link–hinge chain in the vicinity of hinge i shown in Fig. 4b, it is seen that the bending moment is:

$$M_i = k(\alpha_{i-1} - \alpha_i). \tag{8}$$

Substitution of this result into Equation 7 yields the equation which governs the buckling of the link–hinge chain:

$$k(\alpha_i - \alpha_{i-1}) + Pv_i = 0. \tag{9}$$

As the number of elements in the link–hinge chain is increased, the shape of the chain after buckling approaches a continuous curve. Using finite difference methods, a continuous function $f(x)$, which passes through each hinge, can be fitted to the profile of the buckled link–hinge chain. When the number of elements and, therefore, the chain length is allowed to increase without bound at a fixed link size, the chain configuration will conform exactly to the curve traced by the fitted function. It should be noted that the limit of increasing overall chain length at fixed link length is mathematically equivalent to the limit of vanishing link length at fixed overall chain length. Both cases represent the limit of an infinite number of elements.

The details of this procedure are given in Appendix 2. The important result of this analysis is that the curvature of the buckled chain is proportional to the angular change between neighbouring hinges, i.e.

$$(\alpha_i - \alpha_{i-1}) = l\frac{d^2v}{dx^2}. \tag{10}$$

Substituting this result into Equation 9 gives:

$$kl\frac{d^2v}{dx^2} + Pv = 0. \tag{11}$$

Comparison of this equation with Equation 5 shows that the differential equations governing the buckling of the link–hinge chain and continuous column are completely analogous. More importantly, it shows that the bending stiffness of the link–hinge chain is given by the product kl. The dimensions of this product are equivalent to those of the stiffness EI, namely (force) (length)^2.

By analogy, we can write down the critical buckling load for a long link–hinge chain as:

$$P_{cr} = \frac{\pi^2 kl}{L^2}. \tag{12}$$

The validity of using the approximate Equation 12 to predict the critical buckling loads of the link–hinge chain can be demonstrated by comparing values of P_{cr} calculated using Equation 12 with the exact values calculated in Section 3 for several values of p. By noting that $L = pl$, where L is the overall chain length, Equation 12 can be modified to give:

$$P_{cr} = \left(\frac{\pi}{p}\right)^2 \left(\frac{k}{l}\right). \tag{13}$$

This allows a direct comparison between the term

$(\pi/p)^2$ and the coefficient A_p defined in Equation 2. These values are given in Table I. Clearly the agreement is very good even for chains of only six links.

The derived approximate formula. Equation 12, is significant in that it allows calculation of critical buckling loads for a polymer chain (given the imposed assumptions) from bond bending and torsion force constants, bond lengths, and total chain length. It also demonstrates that the bending stiffness of such a chain is a function of the resistance to bond angle deformation and the length of the bonds along the chain axis.

Inspection of Equation 12 will reveal that the buckling loads diminish rapidly with chain length. This result, which neglects the effects of interchain interaction, predicts extremely low compressive strengths for polymer chains of only average molecular weight. As an example, the compressive strength of Kevlar fibres will be calculated using Equation 12.

Because a buckled chain can only support a load which is less than or equal to the critical load, the load required to buckle a collection of non-interacting chains, regardless whether the chains buckle one at a time or all at the same instant, is simply the sum of the buckling loads for each chain. Therefore, the critical stress for buckling a single chain is equal to the buckling stress for any collection of laterally non-interacting chains. A stress calculated in this manner can be used as an estimate of the compressive strength of a fibre having relatively poor lateral strength and stiffness. Typical force constants for bond angle bending are $k = 0.5 \times 10^{-18}$ J rad^{-1} [36]. Most covalent bond lengths are approximately $l \sim 0.1$ nm. The average length of a Kevlar molecule is 210 nm [38] and the cross-sectional area per chain in the unit cell is 0.2024 nm^2 [37]. Using Equation 12, a critical stress of only 0.06 MPa is calculated. This estimate is compared to the measured compressive strength of 700 MPa [5]. Clearly, in order to predict the compressive strength of a fibre formed from a collection of highly oriented and fully extended chains, interchain interactions must be considered.

5. Interchain interactions

The lateral interactions between linear polymer chains in highly oriented fibres are usually secondary bonding forces. For small deviations away from equilibrium separation, these lateral bonds can be adequately modelled with linear springs (again, refer to standard Physical Chemistry texts). Therefore, when a polymer chain is subjected to an axial compressive load, its tendency to buckle and deflect laterally will be opposed by forces which are approximately proportional to the magnitudes of the lateral displacements.

A collection of fully extended and well-oriented chains, that interact as just described, can be treated as elastic columns supported by an elastic foundation. The elastic foundation can be considered as a "matrix" having a stiffness that is the sum of the interactions of all the individual lateral bonds. A method for determining the buckling loads for elastically supported columns using a strain energy approach has been developed by Timoshenko and Gere [30]. Their analysis was applied to a single column supported on only one side by an elastic foundation. The extension of this analysis to the problem of a collection of columns on a foundation has been reported by several investigators as a prediction of the axial compressive strength of unidirectional fibre-reinforced composites [26–29]. A similar analysis will be performed here, following especially the work of Rosen [26], in order to calculate the compressive buckling loads of a collection of link–hinge chains that interact laterally. These loads will be used as theoretical estimates of the axial compressive strengths of oriented polymer fibres.

At the onset of elastic instability, the following energy balance holds:

$$\Delta T = \Delta U_1 + \Delta U_2 \qquad (14)$$

where ΔT is the change in potential energy of the chains due to load P acting to shorten the buckled chains, ΔU_1 the strain energy change of the buckled chains, and ΔU_2 the strain energy change in the elastic foundation. To calculate a critical load, the buckled chains are assumed to take on shapes which produce energy changes that satisfy Equation 14. The smallest load which causes buckling into the allowed shapes is the critical load. Any buckled shape can be described by a series of trigonometric functions which are all periodic over length L. For simplicity it is assumed that the buckled shape of each chain has the same wavelength. Therefore, the only difference between neighbouring chains is a phase mismatch. The two extreme cases considered here are when the chains buckle completely in or out of phase as shown in Fig. 5. These two configurations were called extension and shear mode buckling by Rosen because

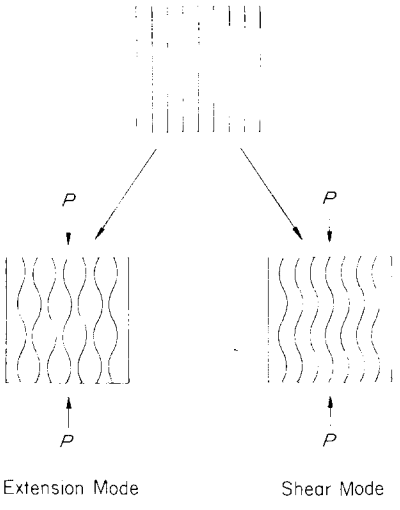

Figure 5 Buckling modes for a collection of link–hinge chains (after Rosen [26]).

of the nature of deformation in the foundation. The details of the calculations of compressive strengths for these two cases are given in Appendix 3.

With the assumption that chain packing produces transverse isotropy (i.e. fibre symmetry), the results obtained for the compressive strengths due to extension mode, σ_c^e, and shear mode, σ_c^s, buckling are:

$$\sigma_c^e = \frac{4\,(E_t kl)^{1/2}}{A} \tag{15}$$

$$\sigma_c^s = G \tag{16}$$

where E_t is the transverse Young's modulus, A the cross-sectional area per chain, and G the longitudinal shear modulus. The values E_t and G are the appropriate elastic constants of the polymer fibre. These quantities appear in the result because it was assumed that bonding between the chains can be modelled with a continuous foundation. Not surprisingly then, these results are similar to those obtained by Rosen, except for the omission of a "volume fraction" term which is meaningless in the present analysis. The predicted compressive strength of a uniaxially oriented polymer is the lower value of the strengths given by Equations 15 and 16.

6. Discussion: calculated and measured compressive strengths

It is unfortunate that data on compressive strengths of highly oriented polymers is scarce. However, a good comparison of the microbuckling theory with measured compressive strengths can be made for oriented polyethylene (PE), Kevlar, graphite and poly(paraphenylene benzobisthiazole) (PBT) fibres. The graphite fibres are included because they are composed of oriented ribbons and microfibrils of "polymeric" graphite [39]. The PBT fibre is based on a lyotropic liquid crystalline polymer and exhibits thermal and mechanical properties similar to those of Kevlar [6]. All four of these fibres have been shown to develop kink bands under axial compression.

To calculate compressive strengths using the microbuckling theory, values of bond bending and torsion force constants, covalent bond lengths, transverse moduli, longitudinal shear moduli and chain cross-sectional areas are required. Covalent bond lengths are generally close to 0.1 nm and bending force constants of valence angles are surprisingly similar for many types of bonds, with values near 0.5×10^{-18} J rad^{-1} [36]. However, for PE it is assumed that bending of the chain will occur almost exclusively by torsion away from the *trans* conformation. A force constant for this torsion in *n*-parafiins was measured to be 0.024×10^{-18} J rad^{-1} [40].

The elastic moduli of these materials have been determined. The longitudinal shear moduli were measured by fibre torsion [5, 6, 41], and the transverse moduli were measured by lateral compression of the fibres [41, 42]. There are no reported values of transverse modulus of PBT fibres, so we estimate a value of 0.5 GPa, which is slightly less than that of Kevlar. The reason for this lower estimated value is that PBT does not hydrogen bond laterally like Kevlar.

Cross-sectional areas were calculated from unit cell dimensions [37, 43–45]. No cross-sectional area or bending stiffness kl can be defined for the graphite ribbons based on the microbuckling model. Therefore, there is no calculation for the extension mode buckling strength of graphite fibres presented here. However, because the shear mode buckling strength is equal to only the shear modulus, this strength can be estimated for the graphite fibres. It is assumed that shear mode buckling of graphite fibres will occur by sliding between graphite basal planes. The shear modulus for this deformation has been determined for dislocation-free graphite to be 4 GPa [46].

Measured compressive strengths of oriented PE are obtained from direct axial compression [14,

TABLE II Calculated and measured compressive strengths of oriented fibres

Fibre	A area per chain (nm^2)	E_t transverse modulus (GPa)	k bending force constant ($\times 10^{18}$ J rad^{-1})	G shear modulus (GPa)	σ^e (GPa)	σ^s (GPa)	σ^{meas} (GPa)
PE	0.18	0.7	0.024	0.6	0.9	0.6	0.04–0.05
PBT*	0.22	0.5	0.5	1.3	2.9	1.3	0.5
Kevlar 29	0.20	0.76	0.5	2.2	3.9	2.2	0.7
Kevlar 49	0.20	0.77	0.5	1.8	3.9	1.8	0.7
Graphite	–	–	–	4.0	–	4.0	2.8

$\sigma^e = 4(E_t kl/A)^{1/2}$, $l = 0.1$ nm.
$\sigma^s = G$.
*PBT = poly (paraphenylene benzobisthiazole)

15]. The compressive strengths of graphite fibres were measured using the elastica test [23]. We have determined the compressive strengths of Kevlar [5] and PBT fibres from measurements of compressive strains to kink formation in both bending and axial compression. By assuming linear elastic behaviour to kink formation, compressive strengths could be calculated from the product of these compressive strains and the respective axial moduli of the fibres. All of these data are summarized in Table II.

In comparing measured and predicted values of compressive strengths, it is clear that the microbuckling theory overestimates the fibre strengths. The best estimates are the shear mode buckling strengths which are lower than the extension mode buckling strengths for all four materials. It is noted that for fibre-reinforced composites with fibre volume fractions greater than 15%, the shear mode buckling strength is also the lower and therefore the more appropriate estimate of compressive strength.

Although the measured compressive strengths are lower than the theoretical estimates (i.e. the shear moduli), the relationship between these quantities is evident. Considering the simplicity of the analysis, which disregards morphological structure, defects and inhomogeneities, the fact that it predicts values within an order of magnitude of measured compressive strengths is indeed remarkable. Theoretical predictions of material strengths are typically two orders of magnitude larger than observed values [47].

Some explanations for the disparity between measured compressive strengths and predicted values will now be discussed. The single chain model was constructed after assuming many simplifications in the specific architecture of the chain. Particular values of bending force constants, bond lengths and bond orientations were ignored. Fortunately, the analysis of a collection of interacting chains showed that the strength is almost exclusively a function of the shear modulus of the foundation and that the bending stiffness of the chains can be neglected when the chains are long. Therefore, if another level of structural scale was considered, for instance long microfibrils, the buckling strength of a collection of these fibrils would also be proportional to the shear modulus. However, studies of kink bands indicate that shear slippage between chains is the mechanism of deformation, so that the present analysis at the molecular level appears valid.

The lateral bonding between chains was modelled as a matrix or continuous foundation having elastic constants equal to those measured for the fibre. Locally, there may be regions where the shear modulus is lower than the measured torsion modulus. Also, there may be anisotropy within the fibre cross-section which would favour buckling within the plane of lowest shear modulus. In these cases the microbuckling strength is determined by the lowest value of shear modulus.

Because predictions of strength are failure analyses (in this case due to microbuckling instabilities), regions which affect the properties of the material locally can possibly lead to a premature failure or buckling. It has been shown that kink bands are nucleated in a localized area at a certain critical stress and then propagate at nearly constant compressive loads [19, 25]. Obviously, lower compressive strengths can result from local inhomogeneities.

The presence of voids in the fibres eliminates the elastic foundation on one side for those chains which line the void surface. Also, chains along the surface of the fibre are supported on only one side. These chains should reach critical buckling loads at a stress equal to half the shear modulus.

Residual stresses have been shown to exist in

graphite fibres [48]. If these stresses are large, regions where the fibre is in compression will reach critical buckling loads sooner than the rest of the material. As with regions surrounding voids, these areas can become nucleation points for kink formation. Some evidence has been seen for the initiation of kink bands near the surface of graphite fibres [24], and the surface of these fibres is apparently under residual compression [48].

Misalignment of chains and microfibrils is seen even in high-modulus fibres [39, 49]. Under axial compression these sections of the fibre will experience shear stresses that could possibly exceed the shear strength between chains or fibrils. In this case, the ultimate compressive strength cannot be predicted by an elastic instability analysis. The compressive strength for materials which fail in shear should be proportional to the shear strength rather than the shear modulus.

Finally, as a point of clarification, it should be emphasized that the classical analysis of elastic buckling instabilities is not a true failure analysis. The purpose of the analysis is to predict the load necessary to *initiate* a geometrical instability for special structures like slender columns. When the critical load is removed from a buckled elastic column, it should return to its original undeformed state. However, because large bending deformations occur at loads slightly greater than the critical loads, true material failure or plastic deformation may occur after buckling is initiated. In this manner, permanent shear deformation can occur after the onset of microbuckling as polymer chains slip past each other to form a kink band, a band which remains after removal of the compressive load. Therefore, the estimate of axial compressive strength for oriented polymers is the load which initiates buckling and subsequent kink formation.

7. Conclusions

The use of a rigid link–elastic hinge chain to model the axial compressive behaviour of extended polymer molecules permits the calculation of a bending stiffness for single chains. This bending stiffness is the resistance of a polymer chain to bending and buckling and it has been shown to be proportional to valence bond bending and bond torsion force constants. For isolated or weakly interacting chains such as in polymer solutions and melts, the model can be used to calculate single chain buckling loads. An example calculation for Kevlar gave an estimated buckling stress of only 0.06 MPa. Flow fields which lead to compression or bending of the polymer chains may result in flow instabilities or even chain scission as a result of severe bending.

Modelling oriented polymer fibres with a collection of interacting rigid link–elastic hinge chains indicates that the compressive strength should be equal to the longitudinal shear modulus. Although the actual compressive strengths are lower than the estimated values, the trend of increasing strength with increasing shear modulus was noted for highly oriented PE, two rigid rod based fibres, and graphite fibres. Several reasons were given for the disparity between predicted and measured compressive strengths, most of which are related to local imperfections in the fibres. All of the explanations point to the relationship between compressive strength and either longitudinal shear modulus or longitudinal shear strength.

Appendix 1. Buckling of a link–hinge chain with three hinges ($p = 4$)

The moment equilibrium is calculated only at hinges labelled 2 and 3 in Fig. 6a. The free-body diagrams for moment balance at these hinges are shown in Fig. 6b. The equations generated by inspection of these diagrams are:

$$\begin{aligned} \Sigma M_2 &= Pl\sin\alpha_1 - k(\alpha_1 - \alpha_2) = 0 \\ \Sigma M_3 &= Pl(\sin\alpha_1 + \sin\alpha_2) - k(2\alpha_2) = 0. \end{aligned} \tag{A1}$$

For small deflections, the small angle approximation $\sin\alpha \approx \alpha$ can be substituted to give:

$$\begin{aligned} (Pl - k)\alpha_1 + (k)\alpha_2 &= 0 \\ (Pl)\alpha_1 + (Pl - 2k)\alpha_2 &= 0, \end{aligned} \tag{A2}$$

or in matrix form:

$$\begin{bmatrix} (Pl-k) & (k) \\ (Pl) & (Pl-2k) \end{bmatrix} \begin{bmatrix} \alpha_1 \\ \alpha_2 \end{bmatrix} = \begin{bmatrix} 0 \\ 0 \end{bmatrix}. \tag{A3}$$

The critical values of P are obtained from:

$$\begin{vmatrix} (Pl-k) & (k) \\ (Pl) & (Pl-2k) \end{vmatrix} = 0 = P^2l^2 - 4klP + 2k^2. \tag{A4}$$

The roots of this polynomial or eigenvalues are given by:

$$P = (2 \pm 2^{1/2})\left(\frac{k}{l}\right). \tag{A5}$$

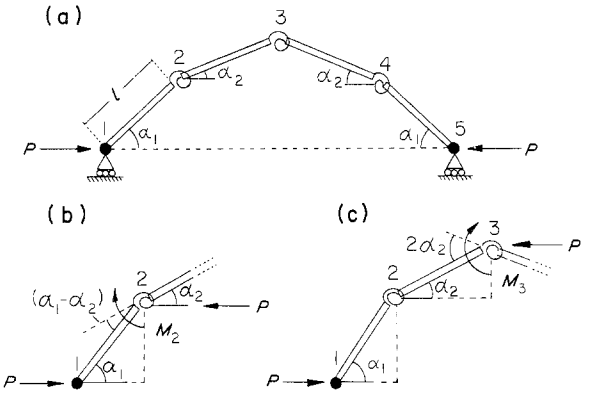

Figure 6 (a) Buckled link–hinge chain ($p = 4$). (b), (c) Free-body diagrams for moment balance.

The critical load is therefore:

$$P_{cr}(p=4) = (2-2^{1/2})\left(\frac{k}{l}\right). \qquad \text{(A6)}$$

It should be noted that a symmetrical buckling pattern was assumed and therefore an equation for hinge 4 would be redundant. The symmetry of the buckling configuration can be proven by assuming a general shape for the buckled chain and determining the eigenvectors, i.e. the values of α_i, for each eigenvalue of buckling load.

Appendix 2. Finite difference method approximation for buckled shape of long link–hinge chains

While a number of finite-difference methods are applicable, we have chosen an interpolation method known as the Backward Newton–Gauss Formula [50]. The first few terms of this formula are given by:

$$f(x_i + r\Delta x) = f_i + r(f_i - f_{i-1}) + \frac{(r+1)r}{2!} \times [(f_{i+1} - f_i) - (f_i - f_{i-1})] + \ldots \qquad \text{(A7)}$$

where: $f(x)$ is a function approximating buckled column shape, x_i the starting point for interpolation, $f_k = f(x_k)$, Δx the equidistant separation of points, i.e. hinges, along x-axis, and r an integer constant.

Mathematically, the links form chords which connect points along the curve $f(x)$. These points correspond to the location of the hinges in the buckled chain. As the number of elements or points increases without bound, the chords and, therefore, the profile of the buckled column will conform exactly to curve $f(x)$.

Referring to Fig. 4b it is easily seen that

$$\Delta x_i = l \cos \alpha_i. \qquad \text{(A8)}$$

With small deflections, $\cos \alpha_i \approx 1$, then:

$$\Delta x_i \approx l \qquad \text{(A9)}$$

and the equidistant separation between hinges becomes:

$$\Delta x = l. \qquad \text{(A10)}$$

The derivatives of the function $f(x)$ at the point $x = x_i$ are obtained by taking the derivatives of Equation A7 with respect to r and then setting $r = 0$. Hence:

$$\Delta x f'(x_i + r\Delta x) = (f_i - f_{i-1}) + \frac{2r+1}{2!} \times [(f_{i+1} - f_i) - (f_i - f_{i-1})]$$

$$\Delta x^2 f''(x_i + r\Delta x) = \frac{2}{2!}[(f_{i+1} - f_i) - (f_i - f_{i-1})] \qquad \text{(A11)}$$

and with $r = 0$:

$$f'(x_i) = \frac{1}{\Delta x}\left\{(f_i - f_{i-1}) + \frac{1}{2!}[(f_{i+1} - f_i) - (f_i - f_{i-1})]\right\}$$

$$f''(x_i) = \frac{1}{\Delta x^2}\{(f_{i+1} - f_i) - (f_i - f_{i-1})\}. \qquad \text{(A12)}$$

It can be seen in Fig. 4b that the differences in parentheses in Equation A12 are given by:

$$(f_i - f_{i-1}) = f(x_i) - f(x_{i-1}) = \Delta v_{i-1}$$

$$(f_{i+1} - f_i) = f(x_{i+1}) - f(x_i) = \Delta v_i \qquad \text{(A13)}$$

Substitution of these results along with Equation A10 into Equation A12 yields:

$$f'(x_i) = \frac{2}{2l}\{\Delta v_{i-1} + \Delta v_i\}$$
$$f''(x_i) = \frac{1}{l^2}\{\Delta v_i - \Delta v_{i-1}\}. \quad \text{(A14)}$$

The increments Δv_i and Δv_{i-1} can also be written as:

$$\Delta v_i = l \sin \alpha_i$$
$$\Delta v_{i-1} = l \sin \alpha_{i-1} \quad \text{(A15)}$$

and for small angles these relations are reduced to:

$$\Delta v_i \approx l\alpha_i$$
$$\Delta v_{i-1} \approx l\alpha_{i-1}. \quad \text{(A16)}$$

Substitution of Equation A16 into Equation A14 gives:

$$f'(x_i) = \tfrac{1}{2}\{\alpha_{i-1} + \alpha_i\}$$
$$f''(x_i) = \frac{1}{l}\{\alpha_i - \alpha_{i-1}\}. \quad \text{(A17)}$$

Rearrangement of the equation for the second derivative gives:

$$lf''(x_i) = l\left(\frac{d^2v}{dx^2}\right)_{x=x_i} = (\alpha_i - \alpha_{i-1}) \quad \text{(A18)}$$

Appendix 3. Buckling of chains on elastic foundations

The chains are assumed to pack in the cross-section of the fibre on a cubic lattice as shown in Fig. 7. The lattice dimension, b, is chosen so that the cross-sectional area per chain b^2 is equal to the value determined experimentally from the actual unit cell of each polymer. The elastic foundation is treated as a "matrix" which surrounds the chains and is not shown in Fig. 7.

Buckling is assumed to be restricted to one of two planes, either xy or xz, which are geometrically equivalent. The foundation is assumed to be equally stiff in the y and z directions. This assumption imposes a restriction of transverse isotropy on the polymer. If the total effect of lateral bonding is summarized as a continuum foundation, then the foundation stiffness in the extension buckling mode is a function of a single transverse modulus, $E_t = E_y = E_z$, and the stiffness in the shear buckling mode a function of a single longitudinal shear modulus, $G = G_{xy} = G_{xz}$. In reality each polymer chain will buckle in a manner that simultaneously minimizes the chain bending strain energy and foundation strain energy changes.

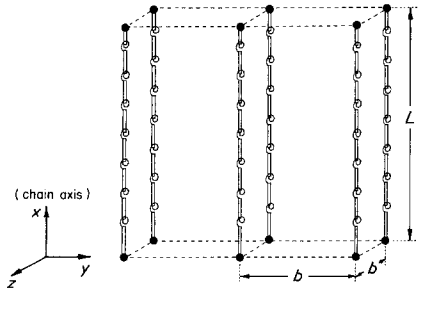

Figure 7 Packing geometry for a collection of interacting and perfectly oriented link–hinge chains.

Rosen postulated that any combination of the two buckling modes will require more energy and therefore higher loads than either of these extremes. The critical load for a material is then given by the lower of the two values predicted for extension and shear mode buckling.

Following Timoshenko and Gere [30], the buckled configuration of any chain can be described by a single series of sine waves. The lateral deflection of a chain is then:

$$v(x) = \sum_n a_n \sin \frac{n\pi x}{L}. \quad \text{(A19)}$$

The change in work due to load P acting on a chain buckled into a configuration given by A19 is:

$$\Delta T = \frac{P\pi^2}{4L}\sum_n n^2 a_n^2. \quad \text{(A20)}$$

The change in bending strain energy due to P acting on a chain with bending stiffness kl is:

$$\Delta U_1 = \frac{\pi^4 kl}{4L^3}\sum_n n^4 a_n^2. \quad \text{(A21)}$$

The strain energy change in the foundation, ΔU_2, must be calculated for each of the two modes of buckling.

A3.1. Extension mode

For buckling within a plane, the extension mode configuration can be depicted as shown in Fig. 8.

The deformation of the foundation is due solely to normal strains given by:

$$\epsilon_y = \frac{2v}{b}. \quad \text{(A22)}$$

The strain energy change is:

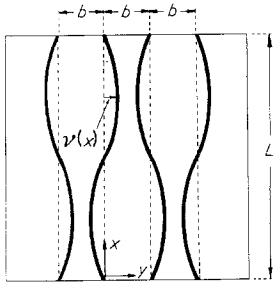

Figure 8 Coordinates for extension mode buckling.

$$\Delta U_2^e = \frac{1}{2}\int_v \sigma_y \epsilon_y \, dV, \qquad (A23)$$

and for a continuum foundation, $\sigma_y = E_t \epsilon_y$, then:

$$\Delta U_2^e = \frac{2E_t}{b^2}\int_v v^2 \, dV. \qquad (A24)$$

The energy change per chain is, therefore:

$$\Delta U_2^e = \frac{2E_t}{b^2}\int_{x=0}^{L}\int_{-b/2}^{b/2}\int_{-b/2}^{b/2} v^2 \, dz dy dx$$

$$= 2E_t \int_0^L v^2 \, dx. \qquad (A25)$$

After substitution of Equation A19:

$$\Delta U_2^e = E_t L \sum_n a_n^2. \qquad (A26)$$

The energy balance is given by substitution of Equations A20, A21 and A26 into Equation 14 yielding:

$$\frac{P\pi^2}{4L}\sum_n n^2 a_n^2 = \frac{\pi^4 kl}{4L^3}\sum_n n^4 a_n^2 + E_t L \sum_n a_n^2 \qquad (A27)$$

solving for P:

$$P^e = \frac{\pi^2 kl}{L^2}\frac{\Sigma n^4 a_n^2}{\Sigma n^2 a_n^2} + \frac{4EL^2}{\pi^2}\frac{\Sigma a_n^2}{\Sigma n^2 a_n^2} \qquad (A28)$$

It was shown by Timoshenko and Gere [30] that ratios of the summations appearing in Equation A28 are minimized when only one arbitrary coefficient a_n is used. Therefore:

$$P^e = \frac{\pi^2 kl}{L^2}(m^2) + \frac{4E_t L^2}{\pi^2}\left(\frac{1}{m^2}\right) \qquad (A29)$$

where $m = 1, 2, 3, \ldots$.

The minimum value of P depends on the relative values of kl and E_t. If the foundation is stiff relative to the bending stiffness of the chain (i.e. $E_t \gg kl$), then the second term in Equation A29 will dominate and large values of m will be required to minimize P. For large values of the integer m, it was shown [30] that:

$$\frac{L}{m} = \pi\left(\frac{kl}{4E_t}\right)^{1/4}. \qquad (A30)$$

Substitution of this result into Equation A29 gives the relationship:

$$P_{cr}^e = 4(E_t kl)^{1/2}. \qquad (A31)$$

For the packing arrangement shown in Fig. 7, the compressive strength estimated for extension mode buckling is then:

$$\sigma_{cr}^e = \frac{P_{cr}^e}{A} = \frac{4(E_t kl)^{1/2}}{A}, \qquad (A32)$$

where $A = b^2$. The result is based on the assumption that the integer, m (which corresponds to the number of half sine waves the columns buckle into), is large. Rearranging Equation A30 to give:

$$m = \frac{L}{\pi}\frac{(4E_t)^{1/4}}{kl}, \qquad (A33)$$

shows that m will take on large values for long chains and for stiff foundations as mentioned earlier.

A3.2. Shear mode

The shear mode of buckling within a plane is represented in Fig. 9. In this case the foundation is only sheared, so the strain energy change is given by:

$$\Delta U_2^s = \frac{1}{2}\int_v \tau_{xy}\gamma_{xy} \, dV, \qquad (A34)$$

and with $\tau_{xy} = G\gamma_{xy}$ for a continuum foundation:

$$\Delta U_2^s = \frac{G}{2}\int_v (\gamma_{xy})^2 \, dV. \qquad (A35)$$

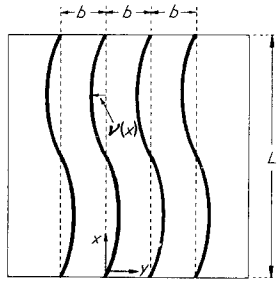

Figure 9 Coordinates for shear mode buckling.

The shear strain is defined by:

$$\gamma_{xy} = \frac{\partial u_y}{\partial x} + \frac{\partial u_x}{\partial y}, \qquad \text{(A36)}$$

where u_y and u_x are the displacements in the y- and x-directions, respectively. The displacements u_y are the lateral deflections of the buckled chain. Since these deflections are independent of the y-direction and since there are no displacements, u_x, Equation A36 reduces to:

$$\gamma_{xy} = \frac{\mathrm{d}u_y}{\mathrm{d}x} = \frac{\mathrm{d}v}{\mathrm{d}x}. \qquad \text{(A37)}$$

Substitution into Equation A34 gives:

$$\Delta U_2^s = \frac{G}{2} \int_{x=0}^{L} \int_{-b/2}^{b/2} \int_{-b/2}^{b/2} \left(\frac{\mathrm{d}v}{\mathrm{d}x}\right)^2 \mathrm{d}z\mathrm{d}y\mathrm{d}x$$

$$= \frac{Gb^2}{2} \int_0^L \left(\frac{\mathrm{d}v}{\mathrm{d}x}\right)^2 \mathrm{d}x. \qquad \text{(A38)}$$

Substitution of Equation A19 into Equation A38 results in:

$$\Delta U_2^s = \frac{\pi^2 b^2}{4L} G \sum_n n^2 a_n^2. \qquad \text{(A39)}$$

Balancing the energies of Equations A21 and A39 with Equation A20 and minimizing the ratios of the summations as before, leaves:

$$P^s = \frac{\pi^2 kl}{L^2}(m^2) + Gb^2 \qquad \text{(A40)}$$

where m is the integer number of half waves of the buckled column. The critical buckling load is simply:

$$P_{cr}^s = \frac{\pi^2 kl}{L^2} + Gb^2. \qquad \text{(A41)}$$

Note that the first term in Equation A41 is the buckling load of an unsupported link–hinge chain, a result derived in Section 4. The additional load required to overcome the support given by the foundation is proportional to the shear stiffness of the foundation. Because the minimum load occurs for $m = 1$, the column will buckle in exactly the same pattern as an unsupported chain; a half sine wave.

For long polymer chains, the first term in Equation A41 can be neglected and the critical load is then:

$$P_{cr}^s = Gb^2, \qquad \text{(A42)}$$

and the corresponding predicted compressive strength is:

$$\sigma_{cr}^s = G. \qquad \text{(A43)}$$

References

1. M. M. SCHOPPEE and J. SKELTON, *Tex. Res. J.* **44** (1974) 968.
2. J. M. GREENWOOD and P. G. ROSE, *J. Mater. Sci.* **9** (1974) 1809.
3. M. G. DOBB, D. J. JOHNSON and B. P. SAVILLE, *Polymer* **22** (1981) 960.
4. T. TAKAHASHI, M. MIURA and K. SAKURAI, *J. Appl. Polymer Sci.* **28** (1983) 579.
5. S. J. DETERESA, S. R. ALLEN, R. J. FARRIS and R. S. PORTER, *J. Mater. Sci.* **19** (1984) 57.
6. S. R. ALLEN, A. G. FILIPPOV, R. J. FARRIS and E. L. THOMAS, Proceedings, 37th Annual Technical Conference, RP/C, SPI, Session 24-B, p. 1, Washington, DC (1982).
7. D. A. ZAUKELIES, *J. Appl. Phys.* **33** (1962) 2797.
8. K. SHIGEMATSU, K. IMADA and M. TAKAYANAGI, *J. Polymer Sci. A2* **13** (1975) 73.
9. G. E. ATTENBURROW and D. C. BASSETT, *J. Mater. Sci.* **14** (1979) 2679.
10. W. L. WU, V. F. HOLLAND and W. B. BLACK, *J. Mater. Sci.* **14** (1979) 250.
11. I. M. WARD, Ed., "Structure and Properties of Oriented Polymers" (John Wiley, New York, 1975).
12. C. J. FARRELL and A. KELLER, *J. Mater. Sci.* **12** (1977) 966.
13. K. IMADA, T. YAMAMOTO, K. SHIGEMATSU and M. TAKAYANAGI, *ibid.* **6** (1971) 537.
14. Y. TAJIMA, Applied Polymer Symposia, No. 27, edited by J. L. White (John Wiley, New York, 1975) p. 229.
15. M. TAKAYANAGI and T. KAJIYAMA, *J. Macromol. Sci. Phys.* **B8** (1973).
16. J. M. DINWOODIE, *J.I. Wood Sci.* **21** (1968) 37.
17. C. T. KEITH and W. A. COTE JR, *Forest Prod. J.* **18**(3) (1968) 67.
18. C. W. WEAVER and J. G. WILLIAMS, *J. Mater. Sci.* **10** (1975) 1323.
19. C. R. CHAPLIN, *ibid.* **12** (1977) 347.
20. A. G. EVANS and W. F. ADLER, *Acta. Metall.* **26** (1978) 725.
21. C. A. BERG and M. SALAMA, *J. Mater. Sci.* **7** (1972) 216.
22. A. S. ARGON, "Treatise on Materials Science and Technology", Vol. 1, edited by Herbery Herman (Academic Press, New York, 1972) p. 79.
23. W. R. JONES and J. W. JOHNSON, *Carbon* **9** (1971) 645.
24. H. M. HAWTHORNE and E. J. TEGHTSOONIAN, *J. Mater. Sci.* **10** (1975) 41.
25. N. C. GAY and L. E. WEISS, *Tectonophysics* **21** (1974) 287.
26. B. W. ROSEN, "Mechanics of Composite Strengthening", ASM Seminar, Philadelphia, Pennsylvania, October (1964).
27. H. SCHUERCH, *AIAA J.* **4** (1966) 102.
28. L. B. GRESZCZUK, *ibid.* **13** (1975) 1311.
29. R. L. FOYE, AIAA Paper No. 66-143, (January, 1966).
30. S. P. TIMOSHENKO and J. M. GERE, "Theory of Elastic Stability" (McGraw-Hill, New York, 1961).
31. J. R. LAGGER and R. R. JUNE, *J. Comp. Mater.* **3**

(1969) 48.
32. J. G. DAVIS JR, PhD thesis, Virginia Polytechnic Institute and State University (1973).
33. B. HARRIS, *Composites* **3** (1972) 152.
34. N. A. PERTZEV and V. I. VLADIMIROV, *J. Mater. Sci. Lett.* **1** (1982) 153.
35. H. MARK, *Trans. Faraday Soc.* **32** (1936) 144.
36. J. P. HUMMEL and P. J. FLORY, *Macromol.* **13** (1980) 479.
37. K. TOSHIRO, M. KOBAYASHI and H. TADOKORO, *ibid.* **10** (1977) 413.
38. L. -S. LI, L. F. ALLARD and W. C. BIGELOW, *J. Macromol. Sci. Phys.* **B22** (1983) 269.
39. R. J. DIEFENDORF and E. TOKARSKY, *Polymer Eng. Sci.* **15** (1975) 150.
40. R. G. SNYDER and G. ZERBI, *Spectrochim. Acta. A* **23a** (1971) 391.
41. D. W. MADLEY, P. R. PINNOCK and I. M. WARD, *J. Mater. Sci.* **4** (1969) 152.
42. S. L. PHOENIX and J. SKELTON, *Tex. Res. J.* **44** (1974) 934.
43. M. G. NORTHOLT and J. J. VAN AARTSEN, *J. Polymer Sci. Polymer Symp.* **58** (1977) 283.
44. E. J. ROCHE, T. TAKAHASHI and E. L. THOMAS, *Amer. Chem. Soc. Symp. Fiber Diffraction Methods* **141** (1980) 303.
45. C. BUNN, *Trans. Faraday Soc.* **35** (1939) 482.
46. O. L. BLAKSLEE, D. G. PROCTOR, E. J. SELDIN, G. B. SPENCE and T. WENG, *J. Appl. Phys.* **41** (1970) 3373.
47. A. KELLY, "Strong Solids" (Oxford University Press, London, 1966).
48. K. CHEN, C. W. LEMAISTRE, J. H. WANG and R. J. DIEFENDORF, 182nd National Conference ACS, New York, Poly 137, August (1981).
49. M. G. DOBB, D. J. JOHNSON and B. P. SAVILLE, *J. Polymer Sci. Polymer Symp.* **58** (1977) 237.
50. C. R. WYLIE and L. C. BARRETT, "Advanced Engineering Mathematics" (McGraw-Hill, New York, 1982).

Received 27 April
and accepted 23 May 1984